

UC Davis

UC Davis Previously Published Works

Title

Combination product of dermal matrix, human mesenchymal stem cells, and timolol promotes diabetic wound healing in mice

Permalink

<https://escholarship.org/uc/item/8bh793z9>

Journal

Stem Cells Translational Medicine, 9(11)

ISSN

2157-6564

Authors

Yang, Hsin-ya
Fierro, Fernando
So, Michelle
et al.

Publication Date

2020-11-01




DOI

10.1002/sctm.19-0380

Peer reviewed

**ENABLING TECHNOLOGIES FOR
CELL-BASED CLINICAL TRANSLATION**

Combination product of dermal matrix, human mesenchymal stem cells, and timolol promotes diabetic wound healing in mice

Hsin-ya Yang¹  | Fernando Fierro^{2,3} | Michelle So¹ | Daniel J. Yoon¹ | Alan Vu Nguyen^{1,4}  | Anthony Gallegos¹ | Michelle D. Bagood¹ | Tomas Rojo-Castro⁵ | Alan Alex⁵ | Heather Stewart³ | Marianne Chigbrow¹ | Mohan R. Dasu¹ | Thomas R. Peavy⁵ | Athena M. Soulika^{1,4} | Jan A. Nolte³ | R. Rivkah Isseroff^{1,6} 

¹Department of Dermatology, University of California, Davis, Sacramento, California

²Department of Cell Biology and Human Anatomy, University of California, Davis, Sacramento, California

³Stem Cell Program, Department of Internal Medicine, University of California, Davis, Davis, California

⁴Institute for Pediatric Regenerative Medicine, Shriners Hospital for Children Northern California, Sacramento, California

⁵Department of Biological Sciences, California State University, Sacramento, Sacramento, California

⁶Dermatology Section, VA Northern California Health Care System, Mather, California

Correspondence

R. Rivkah Isseroff, MD, Department of Dermatology, School of Medicine, University of California, Davis, 3301 C Street, Suite 1400, Sacramento, CA 95816.
Email: rrisseroff@ucdavis.edu

Funding information

California Institute for Regenerative Medicine, Preclinical Development Awards, Grant/Award Numbers: TR2-01787, PC1-08118

Abstract

Diabetic foot ulcers are a major health care concern with limited effective therapies. Mesenchymal stem cell (MSC)-based therapies are promising treatment options due to their beneficial effects of immunomodulation, angiogenesis, and other paracrine effects. We investigated whether a bioengineered scaffold device containing hypoxia-preconditioned, allogeneic human MSCs combined with the beta-adrenergic antagonist timolol could improve impaired wound healing in diabetic mice. Different iterations were tested to optimize the primary wound outcome, which was percent of wound epithelialization. MSC preconditioned in 1 μ M timolol at 1% oxygen (hypoxia) seeded at a density of 2.5×10^5 cells/cm² on Integra Matrix Wound Scaffold (MSC/T/H/S) applied to wounds and combined with daily topical timolol applications at 2.9 mM resulted in optimal wound epithelialization 65.6% (24.9% \pm 13.0% with MSC/T/H/S vs 41.2% \pm 20.1%, in control). Systemic absorption of timolol was below the HPLC limit of quantification, suggesting that with the 7-day treatment, accumulative steady-state timolol concentration is minimal. In the early inflammation stage of healing, the MSC/T/H/S treatment increased CCL2 expression, lowered the pro-inflammatory cytokines IL-1B and IL6 levels, decreased neutrophils by 44.8%, and shifted the macrophage ratio of M2/M1 to 1.9 in the wound, demonstrating an anti-inflammatory benefit. Importantly, expression of the endothelial marker CD31 was increased by 2.5-fold with this treatment. Overall, the combination device successfully improved wound healing and reduced the wound inflammatory response in the

Hsin-ya Yang and Fernando Fierro contributed equally to this study.

This is an open access article under the terms of the Creative Commons Attribution-NonCommercial-NoDerivs License, which permits use and distribution in any medium, provided the original work is properly cited, the use is non-commercial and no modifications or adaptations are made.

© 2020 The Authors. STEM CELLS TRANSLATIONAL MEDICINE published by Wiley Periodicals LLC on behalf of AlphaMed Press

diabetic mouse model, suggesting that it could be translated to a therapy for patients with diabetic chronic wounds.

KEYWORDS

animal models, diabetes, hypoxia, mesenchymal stem/stromal cells (MSCs)

1 | INTRODUCTION

Chronic ulcers in patients with diabetes mellitus (diabetes foot ulcers or DFU) are of increasing concern in the United States. There are over 25 million diabetics in the United States,¹ and approximately 25% of these individuals will develop a foot ulcer during their lifetime.² Even more striking, these ulcers are a causal factor for amputations in about 30% of patients,³ and of these patients with amputations, the 5 year survival rate is estimated at 39% to 68%.⁴ A recent comparison has shown that among deadliest diseases, the 5-year mortality rate for DFU is the same as that of colon cancer (48%).^{5,6} This dire outcome is coupled with extensive US health care expenditures for DFU, of over \$43 billion a year.⁷ Yet, these expenditures for good standard of care result in healing of only 30% of patients with DFU.⁸ This rather dismal cure rate has prompted vigorous research for therapeutic alternatives, and advanced wound care approaches including topical application of growth factors, and extracellular matrix scaffold materials (reviewed in References 9-12). Some of these scaffolds have achieved increased healing in diabetic wounds, as compared with standard of care.^{13,14} These findings suggest that an extracellular matrix scaffold may be a promising base on which to further engineer a wound reparative product.

Indeed, bioengineered living tissue replacements with skin-resident cells embedded within a scaffold that emulates skin compartments have been developed.^{15,16} Currently, there are Food and Drug Administration (FDA)-approved and clinically available medical devices for DFU repair that contain viable fibroblasts (Dermagraft, Organogenesis Inc.), or fibroblasts and keratinocytes (Apligraf, Organogenesis Inc, Canton, Massachusetts).^{17,18} These products have shown modest improvement in healing rates for DFU as compared to the standard of care at 12 weeks (56% with Apligraf vs 38% in control,¹⁷ and 30% with Dermagraft vs 18.3% in control¹⁸). However, no FDA-approved products are composed primarily of mesenchymal stem cells (MSCs), cells that have been demonstrated to direct repair. MSC-based reparative therapies may offer additional advantages over the currently available cellular therapies by modulating the immune and inflammatory response¹⁹ which is aberrant in DFU.²⁰

Allogeneic MSCs isolated from rodents and human have been demonstrated to improve wound closure and re-epithelialization in diabetic mice.²¹⁻²⁴ In limited clinical studies, both autologous and allogeneic MSCs have been examined for their ability to improve healing of DFU.^{25,26} However, there are strong clinical translational advantages for the use of allogeneic MSC: the isolated MSC can be expanded and cryo-preserved to create an optimally therapeutic

Significance statement

Chronic diabetic ulcers are a causal factor for amputations, but the standard of care results in healing of only 30% of patients. This study developed a bioengineered scaffold containing hypoxia-preconditioned, allogeneic human mesenchymal stem cells (MSCs) combined with a beta-adrenergic antagonist, timolol, to treat wounds in diabetic mice. This is the first product that is composed primarily of MSCs with timolol application. The optimized treatment demonstrates promising results of improved healing and decreased inflammation in diabetic wounds. This unique approach provides significant, preclinical evidence supporting the translation of this MSC-based treatment as a therapy for patients with chronic wounds.

master and working cell bank, pre-screened for their pro-reparative secretome, and prepared for clinical applications in a short period of time. Also, allogeneic MSCs have been shown to suppress local immune responses, evade host rejection and persist in the tissue in animal models.²⁷ To capitalize on these advantages, the Integra Matrix Wound Scaffold (MSC/T/H/S) device incorporates bone marrow-derived MSC, which in contrast to MSCs from other sources (placenta, umbilical cord, and adipose), have been very well-characterized and already have a strong safety profile in the clinic.^{28,29} MSCs are embedded and cultured on a cross-linked type I collagen and chondroitin-6-sulfate porous scaffold that supports MSC adhesion and survival (Integra Matrix Wound Dressing) that has FDA-approval.³⁰⁻³⁴ MSCs remain viable *in vitro* when cultivated in this scaffold for at least 15 days, and show limited expansion,³² which allows for a clinical translational regimen of a 7 to 14 day treatment.

In addition, we previously demonstrated 85% of MSCs applied to Integra scaffolds localize to the seeding side and are retained and viable in culture for 15 days.³⁵ Our prior work has also demonstrated that hypoxia pretreatment increases MSC survival *in vivo*,³⁶ which would be predicted to improve cell retention at the wound site in clinical applications. Subcutaneous injection of luciferase-expressing MSCs into immune deficient NSG mice demonstrates that cell retention is enhanced when the MSCs are preconditioned under 1% hypoxia for 48 hours.³⁶ The hypoxic preconditioning decreases glucose

consumption,³⁶ thus resulting in longer survival in nutrient-deficient environments.

The inclusion of timolol as a preconditioning element derives from our prior body of work has demonstrated that wound tissues can generate catecholamines^{37,38} and that these catecholamines can impair healing by inhibiting keratinocyte migration and wound epithelialization,³⁷⁻⁴⁰ altering fibroblast reparative phenotype,^{41,42} and sustaining an inflammatory environment within the wound by increasing neutrophil dwell times⁴³ and by increasing inflammatory cytokines within the wound.⁴³ The beta adrenergic antagonist, timolol, a drug that is FDA-approved and clinically used with topical delivery for wide-angle glaucoma, has been shown to reverse these deleterious catecholamine effects, and thus improve healing in multiple *in vitro*, *ex vivo*, and *in vivo* wound models.^{37,39,40,43} Importantly, we have also demonstrated that timolol pretreatment, abrogates epinephrine, and bacterial TLR activators induced IL-6 secretion by MSCs.⁴⁴

These critical findings underpin our decision to incorporate MSCs preconditioned with both hypoxia and timolol into an extracellular matrix scaffold material. Here, we report the bioengineering of the MSC/T/H/S combination device and its efficacy and immunomodulatory effects in an impaired healing, diabetic murine wound model. We believe this is a unique approach that may provide superior healing responses in patients with diabetic wounds.

2 | MATERIALS AND METHODS

2.1 | MSC source

Fresh bone marrow aspirates were purchased from Stem Express (Placerville, California) from five healthy donors. MSCs were isolated using a Ficoll density gradient (Sigma-Aldrich, St. Louis, Missouri) and based on their adherence to plastic.³⁶ Cells were cultured in DMEM with 10% fetal bovine serum (FBS, Atlanta Biologicals, Flowery Branch, Georgia) and then expanded to up to passage 4 and cryopreserved. Full characterization of cells is presented in Supplementary Table 1 and Supplementary Figures 1-5.

2.2 | MSC/timolol/hypoxia/scaffold device preparation

Five days prior to wounding, MSCs were thawed, washed, and seeded on 8 mm circular matrix scaffolds (Integra-Wound Matrix, catalog # 54051T, Integra LifeSciences, Plainsboro, New Jersey, 0.5 mm thickness, trimmed to the same sizes as the wounds) for 4 hours to overnight. Integra (catalog # 52025, 1 mm thickness) was used in Figure 1C, which resulted in a slightly lower rate of healing. The MSC-Integra scaffolds were then incubated in 1 μ M timolol at 1% Oxygen (hypoxia) in the MSC culture medium at 37°C for at least 48 hours, before being sealed in the culture medium in a hypoxic chamber and transferred to the surgery room.

2.3 | Mouse model

Db/db mice (#00642 Wildtype for Dock^{7m}, Homozygous for Lepr^{db}, 8-10 weeks old females from Jackson lab, Sacramento, California) were used at 12 to 14 weeks. The mouse wounding protocol is approved by the UC Davis IACUC (#20111) and is in accordance with all AAALAC guidelines. The mouse weight (40-50 g) and blood glucose (tested by the LifeScan OneTouch Ultra Blue Meter, Johnson and Johnson, New Brunswick, New Jersey) were monitored for 1 to 2 weeks to confirm the blood glucose level was >200 mg/dL. Mice that lost more than 20% weight during the experiments were excluded. The final results were combined from 6 to 10 mice/treatment in three repeated experiments.

2.4 | Wounding surgery and implanting scaffolds

The dorsal surface of the mice was shaved 24 hours before surgery. The mice were anesthetized with 2.5% isoflurane, the weight and blood glucose were measured again, and analgesic (Buprenex, 0.05 mg/mL, 1 μ L/g body weight) was injected subcutaneously. After betadine and alcohol washes of the mouse dorsum, two sterile silicon splints (10 mm inner diameter, 16 mm outer diameter, 1.6 mm thick) were glued (Superglue, 3M, Minnesota) at 35 mm from the base of the skull, and 10 mm on either side of the spine on each mouse and secured with eight sutures (6-0 Ethilon, #697G). A 6-mm full-thickness, circular wound was created in the center of each splint by a biopsy punch and surgical microscissors, as we have described⁴⁵ (Figure 1A, day 0). The MSC/T/H/S scaffold device was removed from culture medium and inserted into the wound bed with the cell-application side facing down. A 16-mm circular plastic coverslip was applied on top of the splint and the wound area was sealed with a transparent, semi-permeable dressing (Tegaderm, 3M, Maplewood, Minnesota). The wounds were monitored daily and the coverslips and transparent dressings were replaced every 3 days. Daily timolol treatment was injected into the space between the wound bed and the coverslips.

2.5 | Topical administration of timolol

Derivation of the dose to apply topically to the wound was calculated from FDA-approved dosing schedules for glaucoma of 0.5 mg/day (1 drop of 0.5% solution/eye/twice/day, or 50 μ L \times 0.5% \times 1 eye \times 2 applications per day.⁴⁶ For equivalent dosing of the wound, 0.047 mg timolol/6-mm wound, or 50 μ L of 2.9 mM timolol solution per wound was used (Supplementary Methods).

2.6 | Wound tissue and blood collection

Wound tissue was collected on day 7 (Figure 1A). The Tegaderm, coverslips, sutures, and splints were removed and a 1 \times 1 cm² section of

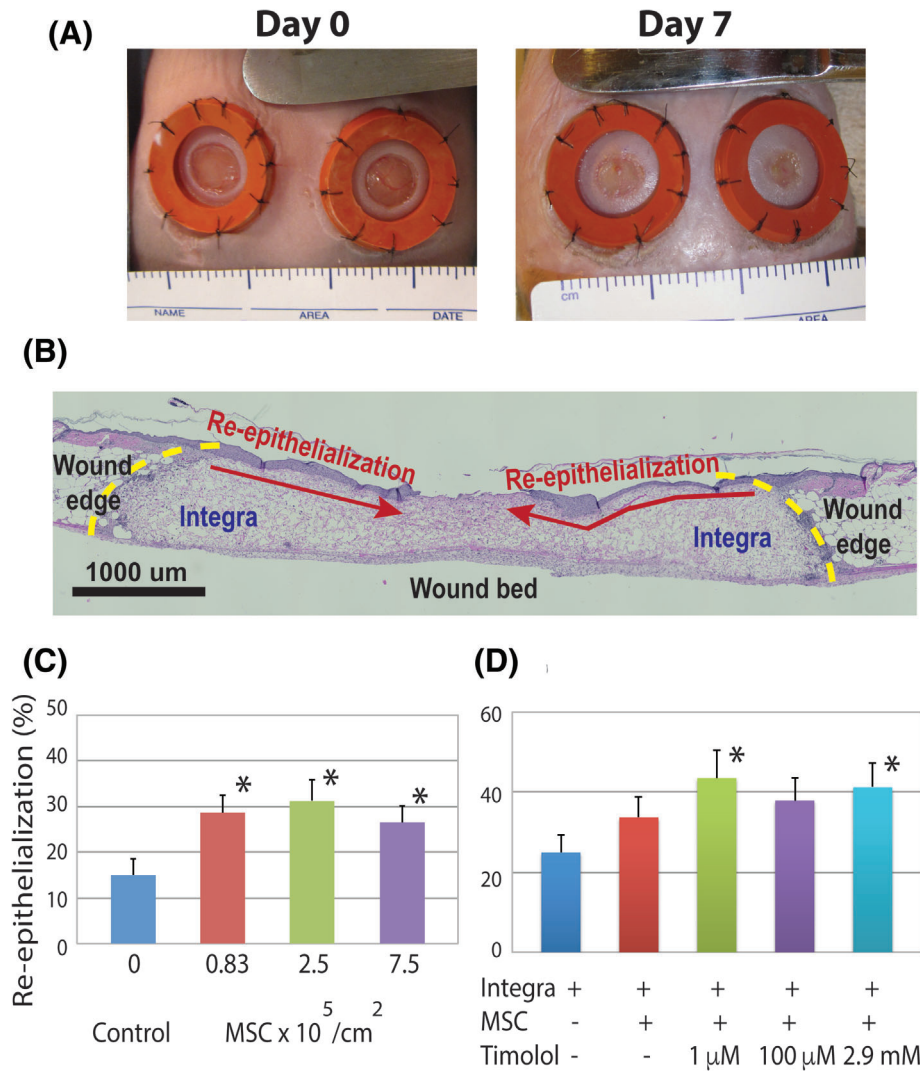


FIGURE 1 The combined treatment of MSC and timolol improves wound healing in diabetic mice. A, in vivo wounding assay. Bilateral 6 mm skin excisional wounds were made with splints to reduce skin contraction (left panel, day 0) and the different treatment matrices were inserted to the wound beds (right panel, day 7). B, Quantitation of wound healing. A representative image of H&E staining of the day 7 wound is shown. The original wound edge (yellow dashed lines) on each side is determined by the absence of subdermal adipose tissue. Re-epithelialization (red arrows) is defined by epithelial cell growth above the Integra matrix (scale bar = 1000 μm). C, MSC embedded in Integra improve wound healing. The mouse wounds were treated with different concentrations of MSCs seeded on Integra and collected on day 7. All the MSC-Integra scaffolds significantly improved wound epithelialization by more than 70% relative to the Integra alone group ($*P < .05$ as compared to the Integra control). D, Timolol increases wound healing. Treatment of wounds post-implantation of MSC-Integra scaffolds with either 1 μM or 2.9 mM timolol increased wound re-epithelialization as compared to nontimolol treated controls (mean \pm SEM, $n = 12$ wounds from six mice in each group, $*P < .05$)

skin tissue around the wounds was excised and fixed in 4% paraformaldehyde for 24 hours for histological analysis. Blood was collected by cardiac puncture for HPLC analysis (Supplementary Methods).

2.7 | Quantitation of wound healing

After fixation, the wound tissue was paraffin-embedded, sectioned to 5 μm and H&E stained for determination of wound re-epithelialization. All the histological sections were imaged using a BioRevo BZ-9000 inverted microscope (Keyence, Osaka, Japan) and measured by an investigator blinded to treatment group with the BZ-II viewer and analyzer (Keyence, Japan). The wound edges were defined by the absence of underlying adipose tissue and wound healing is determined by the re-epithelialization of the epidermis layer.^{47,48} The outgrowth of the newly formed epidermis was tracked manually from the wound edges and the percentage of the combined length of the re-epithelialization to the total length of the wounds was calculated (Figure 1B-D). Two-tailed Student's *t* test was performed to determine statistical differences between the treatment groups.

2.8 | Quantitation of plasma timolol concentrations

An ultra-sensitive HPLC (UHPLC, Antec Scientific, Zoeterwoude, the Netherlands) with UV-Visible absorbance detection at 284 nm (Antec neurotransmitter analyzer) was used to detect timolol. Timolol was quantitated with the lower limit of quantitation (LOQ) of 3.0 ng/mL (Supplementary Methods). Plasma samples from 6 db/db mice were examined in each treatment group.

2.9 | Quantitative PCR for cytokine expression

The mouse wound tissue was collected on day 3 post wounding, stored in RNALater (Invitrogen, Carlsbad, California) at 4°C, and homogenized using a Tissue Tearor homogenizer (Biospec, Bartlesville, Oklahoma) in the Qiazol Lysis Buffer (Qiagen, Venlo, the Netherlands). RNA was isolated with RNeasy Mini Kit (Qiagen) and quantitative PCR was performed (Supplementary Methods). Each sample was run in duplicate and mRNA levels of target genes were

normalized to the reference gene, TBP. Fold change of the target genes as normalized to normal skin was determined by $2^{(-\Delta\Delta Ct)}$ ($\Delta\Delta Ct = \Delta Ct_{(target - reference)}$ of sample $- \Delta Ct_{(target - reference)}$ of normal skin). Each fold change dataset was analyzed by the Grubbs Tests to remove outliers and by Student's *t* test to determine statistical significance.

2.10 | Immunophenotyping the wound tissue

The mouse wound tissue was digested in the 0.4 U/mL Dispase II (2 hours, 37°C) and 1 mg/mL Collagenase D (30 minutes, 37°C) in RPMI 1640 containing 10% FBS, and 50 μ M beta-mercaptoethanol, and the digestion was stopped by 10 mM EDTA. The cell suspension was filtered with 100 μ m cell strainers to remove tissue debris. Red blood cells were removed via ammonium-chloride-potassium lysis. Before immunostaining, Zombie Red viability dye (Biolegend, San Diego, California) was added to all cells, and Fc receptors were blocked with anti-CD16/32 (BD Biosciences, Franklin Lakes, New Jersey). Myeloid cells (neutrophils, monocytes and macrophages) were stained with Brilliant Violet (BV)-711 conjugated anti-mouse CD11b antibodies, and peridinin chlorophyll protein (PerCP) conjugated anti-mouse CD45 antibodies (Biolegend). Within the myeloid population, neutrophils were labeled with FITC or BV510 conjugated anti-mouse Ly6G antibodies (BD Biosciences and Biolegend), inflammatory M1 monocytes/macrophages were stained with phycoerythrin (PE) conjugated anti-mouse Ly6C, and allophycocyanin Fire 750 conjugated anti-mouse MHCII (Biolegend) and anti-inflammatory M2 monocytes and macrophages were stained with BV421 conjugated anti-mouse CD206 (Biolegend). Cells were analyzed by an Attune flow cytometer (Life Technologies, Carlsbad, California). The gating strategy for neutrophils and macrophages is shown in Figure 4A-C,G. Live cells were selected with Zombie red and immune cells were identified by the CD45+. Neutrophils were identified as Ly6G+ CD11b+ and monocytes/macrophages were identified as Ly6G- CD11b+ (Figure 4B,C). M1 and M2 monocytes/macrophages were further identified with Ly6C and CD206. M1 cells are Ly6C+ and M2 cells are CD206+ (Figure 4G).

2.11 | Analysis of wound angiogenesis

Wound tissue sections were de-paraffinized, rehydrated, subjected to heat mediated epitope retrieval (Tris/EDTA, pH 9; Agilent DAKO, 25 minutes at 95°C), and blocked (0.1% Triton X-100, 1% BSA in PBS, 90 minutes) prior to incubation with Anti-CD31 or the isotype control (Rabbit polyclonal antibodies, Ab124432, Abcam, Cambridge, Massachusetts; Rabbit IgG polyclonal Isotype Control, Abcam Ab171870) followed by secondary antibody conjugated to Dylight 649 (1:200, Goat anti-rabbit IgG; Vector Laboratories, Burlingame, California). Sections were mounted with ProLong gold antifade mountant with DAPI (Thermo Fisher Scientific, Waltham, Massachusetts) and imaged with a confocal laser scanning microscope (Olympus Fluoview FV10i), and the CD31 fluorescence was analyzed by an investigator blinded to

treatment group with Volocity software (PerkinElmer, Waltham, Massachusetts). The wound bed area between the wound edges and below the implanted MSC/matrix device was selected as region of interest, intensity threshold was determined by histogram in each image to include all the fluorescent signals, and the fluorescent objects sized between 10 and 300 μ m² were counted and averaged to the wound bed area. An ANOVA test was performed to determine statistical significance.

3 | RESULTS

3.1 | MSC screening from donors

Bone marrow aspirates from five different donors were purchased from a commercial vendor. Processing details are given in Supplementary Table 1, and vials of P1, and P2 were cryo-preserved as the Master Cell Bank (MCBs). A single P2 vial of each MCB was thawed and used for testing sterility (bacterial, mycoplasma and endotoxin levels), secretion of pro-regenerative signals by enzyme-linked immunosorbent assays (ELISAs), proliferation, multipotent differentiation potential, karyotype stability, expression of surface markers and ability to promote endothelial cell migration.

ELISAs of MSC conditioned medium were used to determine the expression levels of key factors secreted by MSCs that could impact wound repair, including Angiogenin, Angiopoietin-2, Transforming Growth Factor β 1 (TGF- β 1), Interleukin 8 (IL-8), Vascular Endothelial Growth Factor (VEGF), Wnt4, and serotonin. Results of these measurements are shown in Supplementary Figure 1 and summarized in Supplementary Table 1, as are proliferation rates (all five batches showed comparable cell growth).

The master banks MSCWT3 and MSCWT5 selected to generate the working cell bank (WCB) due to their similarity in secretion profile also showed the same proliferation rate, with population doubling (PD) rate of 0.66 per day (Supplementary Methods). Cell purity measurements determined that all five MSC batches had less than a 0.2% CD45⁺ and consistently expressed all MSC markers tested (CD73, CD90, and CD105). All batches of MSCs exhibited tri-lineage differentiation potential as determined using the respective differentiation assays⁴⁹ (Supplementary Figure 4), and all batches of MSCs showed the normal male karyotype (46, XY), tested by UC Davis Karyotyping Core.

Functional assays were used to test the ability of all five MSCWT batches for their ability to promote migration of endothelial cells. Conditioned medium from all five MSC batches significantly induced migration of human umbilical vein endothelial cells in a wound/scratch assay (Supplementary Figure 5).

Although the five tested MCB batches showed substantial similarities, the secretion profile of key factors was variable. In consequence, we chose the two MCBs (MSCWT3 and MSCWT5) with the most similar profiles for the generation of the WCBs. Cells from these two WCBs were then exclusively used for all experiments described below.

3.2 | Optimization of MSC and timolol concentrations

We compared several MSC concentrations seeded on the dermal matrices to determine the optimal MSC dosing in the diabetic mouse wound model (Figure 1A without additional timolol treatment, or with

post-operational timolol treatment (Figure 1B). Analysis of wound re-epithelialization (Figure 1C, day 7 tissue) suggests that the MSC-containing scaffolds embedded with 0.83 , 2.5 and 7.5×10^5 cells/cm², significantly improved wound epithelialization by 90%, 108% and 77% at respectively (n = 12 wounds from 6 db/db mice, $P < .05$) when compared with matrix (Integra) alone. Therefore, we chose to

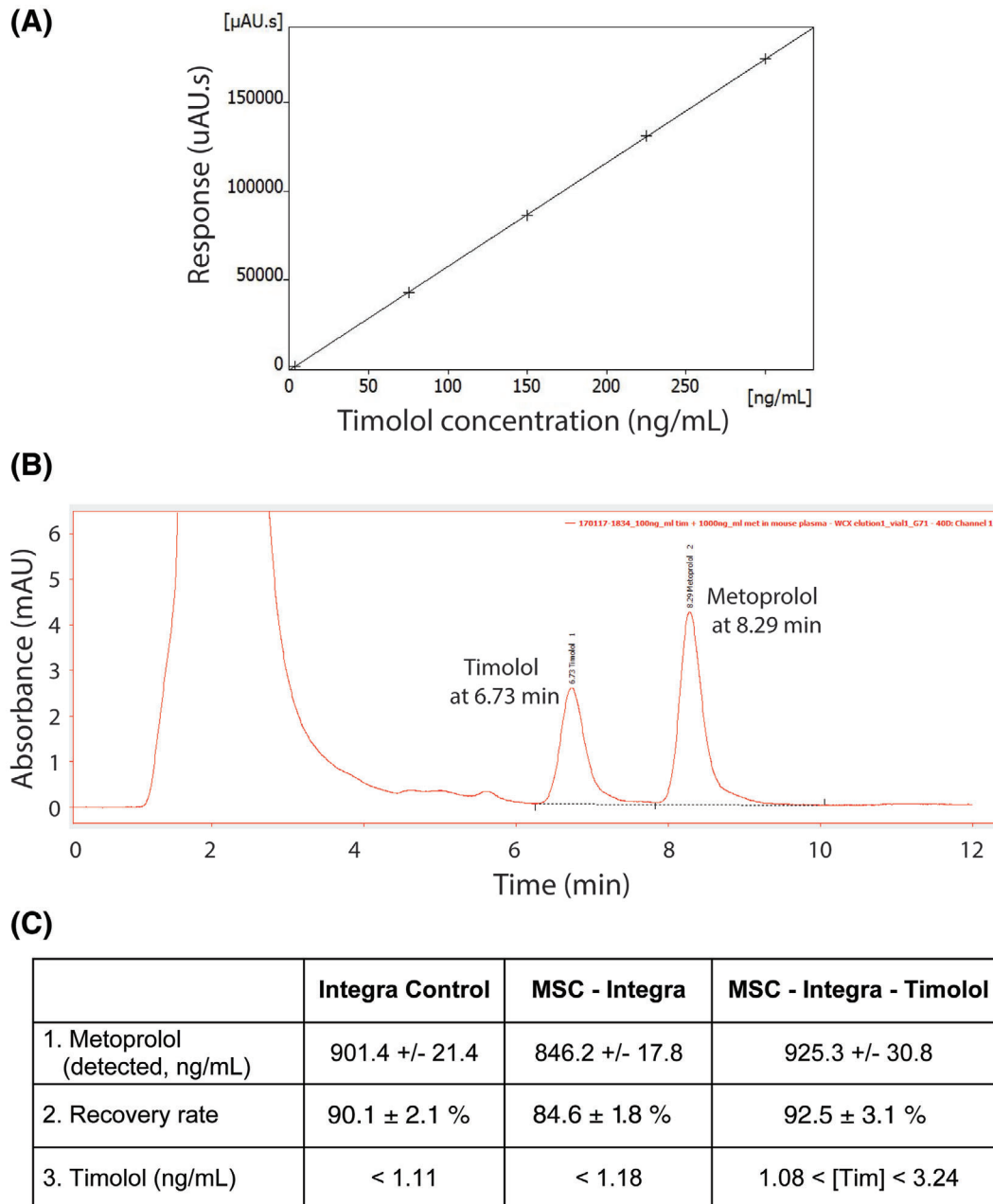


FIGURE 2 Quantitation of systemic absorption of timolol. A, Timolol standard curve by UHPLC. A standard curve for UHPLC was prepared with 3 to 300 ng/mL. The lowest value 3 ng/mL of the standard curve is the limits of quantitation (LOQ). B, Timolol and metoprolol peaks in an UHPLC chromatograph. Timolol (100 ng/mL) and metoprolol (1000 ng/mL, control) were added to the untreated mouse plasma, extracted and detected by UHPLC. The retention time of timolol is 6.7 and 8.3 minutes for Metoprolol. One ng/mL is the limits of detection (LOD) or the minimal visible peak in the chromatograph. Any values between 1 and 3 ng/mL (between LOD and LOQ) are considered detectable, but not quantifiable. C, Plasma timolol concentrations. The mouse blood samples were collected on day 7 and examined by UHPLC. Metoprolol (1000 ng/mL) was added as internal standard. The daily accumulative timolol dose is 0.092 mg/mouse, but the detected timolol concentrations are extremely low (mean ± STDEV, n = 6 mice in each group)

continue investigations using the optimized MSC concentration of 2.5×10^5 cells/cm² in the MSC/T/H/S device.

To determine the optimal concentration for the daily treatment of timolol post application of the MSC/T/H/S device to the wound, timolol solution (1 μ M, 100 μ M, and 2.9 mM, 50 μ L/wound) or PBS (control) was applied daily from day 0 until the day before tissue collection. Both the 1 μ M and 2.9 mM timolol treatments showed a significant increase (Figure 1D, 74.9% improvement with 1 μ M and 65.6% with 2.9 mM timolol, $n = 12$ wounds of 6 db/db mice, $P < .05$) in wound re-epithelialization as compared to the control group (Integra alone). There were no statistical differences between percentages of healing with 1 μ M and 2.9 mM. Since 2.9 mM is the concentration derived from the approved clinical dosing of 0.5% timolol for glaucoma (see Supplementary Methods), we chose this concentration as the optimized dose. The trend for improved healing is sustained with the MSC/T/H/S treatment at 14 days, however the statistical significance to a P value of $<.05$ was not attained on the day 14 samples (Supplemental Figure 6).

3.3 | Systemic absorption of timolol

Oral and corneal administrations of timolol are approved by the FDA, but the systemic absorption through an open skin wound has not yet been evaluated. To determine the accumulated plasma concentration of topically applied timolol, mouse blood was collected and analyzed by UHPLC after 7 days of treatment. Standard curves of metoprolol and timolol (Figure 2A) were established in each experiment.

Timolol was eluted at 6.7 minutes (Figure 2B, 100 ng/mL Timolol added to mouse plasma for calibration) and the metoprolol retention time is 8.3 minutes (Figure 2B, 1000 ng/mL added). Timolol concentrations in mouse plasma with the topical treatment were detectable but below the LOQ (Figure 2C, MSC-Integra-Timolol, 1 ng/mL $<$ Timolol concentration in plasma $<$ 3 ng/mL), suggesting that the accumulated levels of timolol in circulation after a 7-day topical treatment is minimal.

3.4 | Cytokine modulation

During the short-term stem cell therapy (7-14 days), MSCs likely do not differentiate to repair the damage tissue.^{19,50} Instead, MSCs secrete cytokines to modulate reparative cellular functions. We examined cytokine expression in wound tissue on day 3 post wounding. Among these cytokines, the change in the C-C motif chemokine ligand 2, CCL2, is particularly noteworthy (Figure 3A). CCL2, a chemokine identified in MSC extracellular vesicles,⁵¹ recruits monocytes, memory T cells, and dendritic cells.^{52,53} A recent study has shown that CCL2 concentration is decreased in diabetic wounds and topical application of CCL2 improved the delayed healing in diabetic mice.⁵⁴ Here, we observed a similar effect, in that when the diabetic wounds healed with the MSC/T/H/S device treatment, the CCL2 expression level in

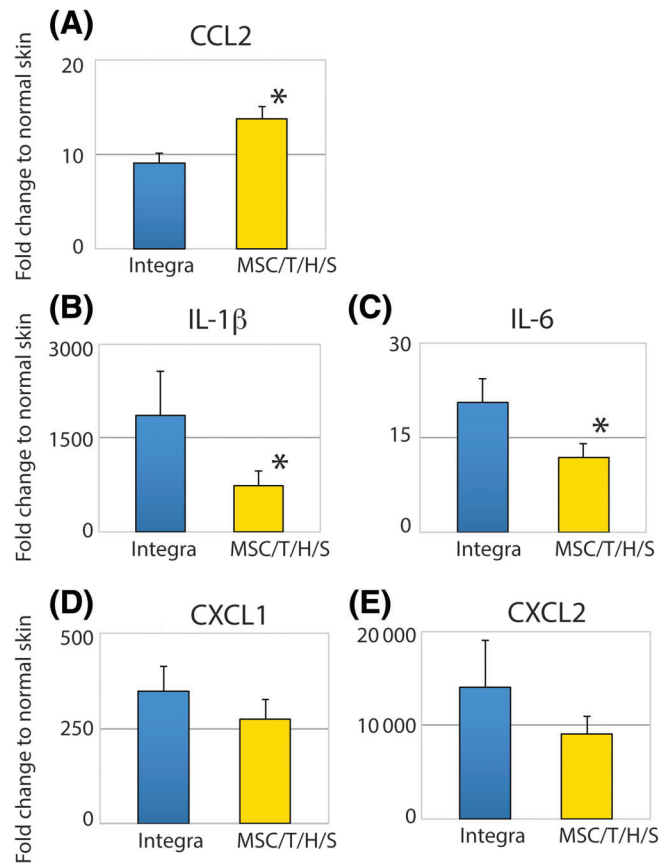


FIGURE 3 The MSC/T/H/S treatment decreases expression of inflammatory cytokines in mouse wounds. The relative amounts of cytokine mRNA on the day 3 wounds were measured by quantitative PCR and normalized to unwounded mouse skin. A-C, CCL-2, IL-1 β , and IL-6 decreased significantly with the MSC/T/H/S treatment when compared with the Integra control ($*P < .05$). D,E, CXCL-1 and CXCL-2 show a trend of decreasing, but the fold changes are not statistically significant (mean \pm SEM, $n = 12$ wounds from six mice)

the wound tissue was also significantly elevated compared to the control treatment (Figure 3A).

Two of the pro-inflammatory cytokines, interleukin 1 beta (IL-1 β) and interleukin 6 (IL-6)⁴³ were significantly decreased in the MSC/T/H/S device treated wounds (Figure 3B,C), supporting its immunomodulatory functions. CXCL1 and CXCL2 are ligands for CXCR2 and promote neutrophil migration to the wound site. CXCR2 has been known to mediate impaired healing in senescence and diabetes.^{55,56} Both the CXCL-1 and CXCL-2 trended downward in the MSC/T/H/S device treated wounds (Figure 3D,E). These results suggest that this treatment decreases inflammation in the early wound, and likely is one of the mechanisms by which wound healing is improved with this treatment protocol.

3.5 | Modulation of wound immunophenotype

To characterize the in vivo immune responses to the MSC/T/H/S device treatment, single cells isolated from wounded tissues were

examined by flow cytometry. Neutrophil infiltration is an early event and associated with the inflammatory phase of wound healing and was significantly decreased in the treated wounds (decrease in total CD45+ immune cells at wounds by 38.8%, Figure 4A,D, $P < .05$). Although the percentage of the neutrophils was similar across all treatments (Figure 4E), the absolute neutrophil counts on day 4 post-injury were decreased by 44.8% in the device treated wounds as compared to the control (scaffold alone) (Figure 4F, 4.86×10^5 cells in control vs 2.68×10^5 cells with the treatment; $P < .05$). In addition, pro-inflammatory monocyte-derived macrophages (M1) are also present during the early stages of wound healing contributing to the inflammatory environment of the wound.⁵⁷ As the wound heals, the local macrophage population transitions toward the anti-inflammatory/pro-repair (M2) phenotype.⁵⁷ The relative percentage of pro-inflammatory M1 (Ly6C+) macrophages was decreased (Figure 4H, left panel, 44% in control vs 32% in the device treated wounds, $P < .05$), whereas there were no significant changes in the relative percentages of anti-inflammatory/pro-repair M2 macrophages (Figure 4H, middle panel, 22% in control vs 31% in treated). These

changes result in a shift of the M2/M1 ratio from 1 in the scaffold control wounds to 1.9 with MSC/T/H/S device treated wounds (Figure 4H, right panel) on day 4 post-injury. The resultant decrease in pro-inflammatory cells during the early phase of healing likely minimizes the subsequent inflammatory sequelae and promotes wound re-epithelialization.

3.6 | Modulation of wound angiogenesis

Mouse wound tissues collected on day 7 were processed for immunofluorescence staining for the endothelial cell/angiogenesis marker CD31. CD31 immunoreactivity was mostly observed in the wound bed (Figure 5A-D, CD31 in red). Quantification of CD31 fluorescence signals at the wound bed shows that CD31 immunoreactivity in the MSC/T/H/S device treated wounds was increased by 256% when compared with the control (Integra only, Figure 5E, $P < .05$). These results suggest that applying the device to the wound improves angiogenesis during wound healing.

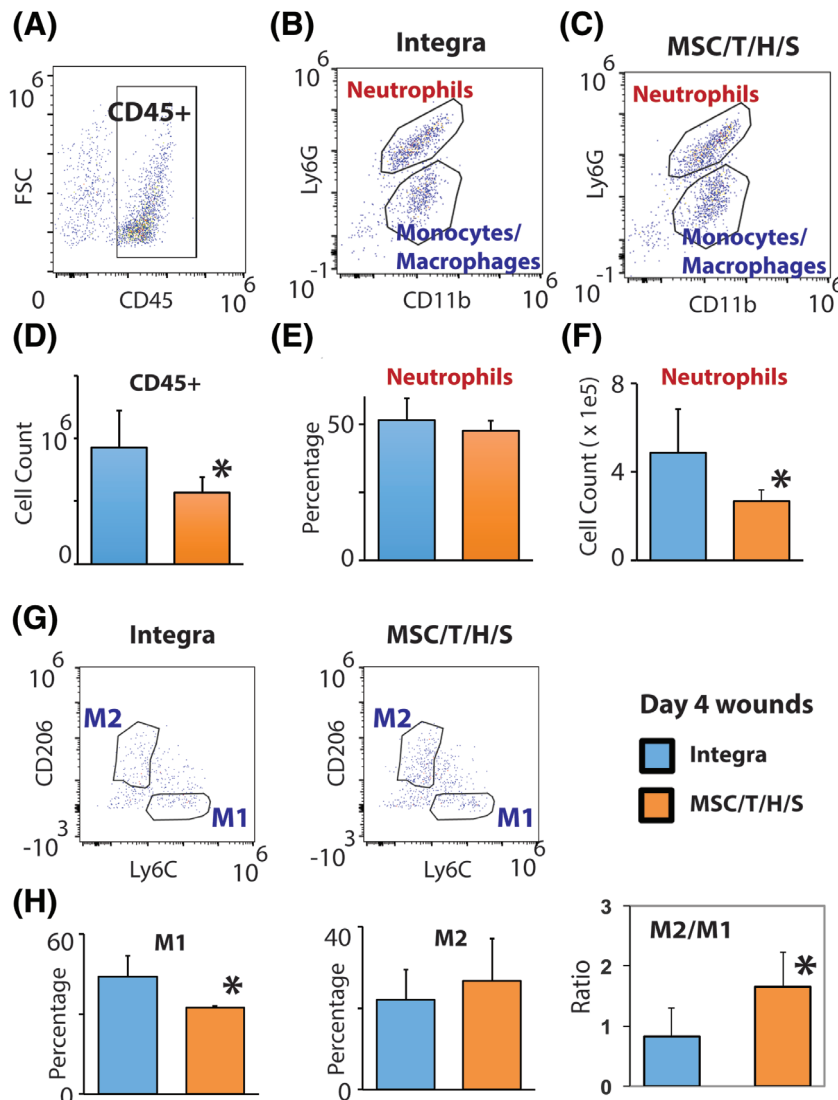


FIGURE 4 The MSC/T/H/S treatment decreases neutrophil numbers and shifts macrophages to M2. A-C,G, Gating strategy to identify neutrophils, monocytes, and M1 and M2 macrophages. D-F, Quantification of cell populations. H, Shift of macrophages from M1 to M2 phenotype. Representative dot plots to show the gating strategy in flow cytometry in A. Live cells were selected with Zombie red and the immune cells were identified by the CD45+ population. Neutrophils were identified as Ly6G+ CD11b+ and monocytes/macrophages were identified as Ly6G- CD11b+ in B,C. The CD45+ immune cells were decreased with the MSC/T/H/S treatment in D (* $P < .05$). Panels E and F were gated in Ly6G- CD11b+ neutrophil cells. Decreased numbers of neutrophils are found in the wounds treated with MSC/T/H/S compared to Integra controls on day 4 post injury in F (* $P < .05$). M1 and M2 monocytes/macrophages were further subclassified as M1 cells (Ly6C+) and M2 cells (CD206+) in G. On day 4, the percentages of pro-inflammatory M1 macrophages (Ly6C+) are decreased and the M2/M1 ratio increased with the MSC/T/H/S treatment when compared to controls (Integra alone) in (H) (* $P < .05$, mean \pm STDEV, $n = 10$ wounds from five mice)

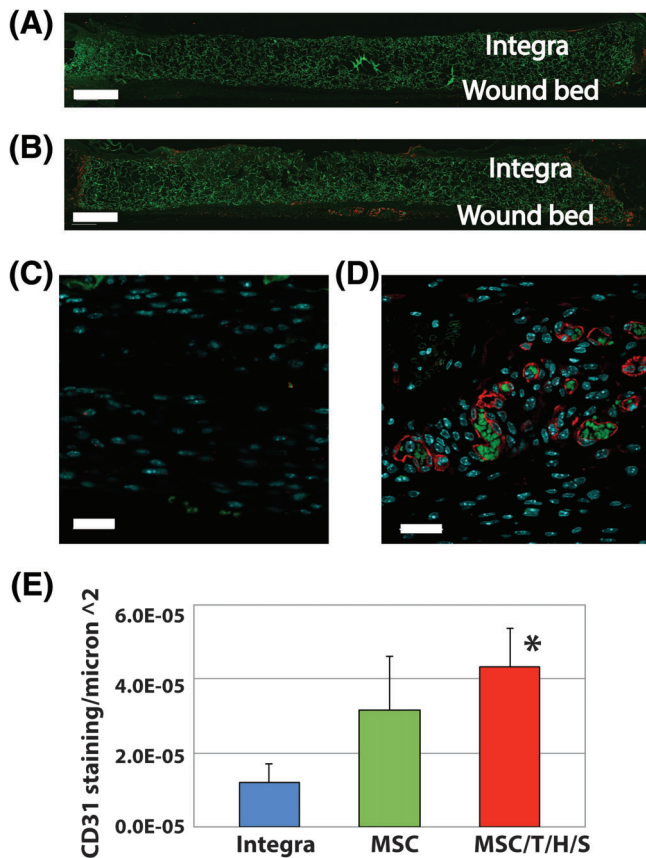


FIGURE 5 Quantitation of angiogenesis. Anti-CD31 staining across the entire wound section of day 7 mouse wounds with, A, Integra control and, B, MSC/T/H/S treatments (scale bar = 500 μ m). CD31 signals are in red, nuclei in blue, and red blood cells in green in the higher magnification ($\times 60$) images with, C, Integra control and, D, MSC/T/H/S treatments (scale bar = 25 μ m). E, Quantification of the CD31 signals (CD31 positive objects/ wound area) in each treatment groups. The MSC/T/H/S treatment significantly increased the CD31 staining at the wound bed (* $P < .05$, mean \pm STDEV, $n = 12$ wounds from six mice.)

4 | DISCUSSION

Our goal was to engineer a MSC-based cellular device optimized to improve healing in diabetic wound by combining elements with known pro-reparative functions. The optimized device combines hypoxic preconditioning of MSC and beta adrenergic blockade with timolol, prior to their incorporation into an extracellular matrix scaffold for dermal regeneration. The optimization protocols were tested in an impaired wound healing model in diabetic db/db mice. The db/db mouse is widely used to model impaired healing in diabetes, despite some of its shortcomings, primarily that the type 2 diabetes (T2D) in the model is a function of a leptin receptor mutation, that is not the primary pathogenesis of T2D in humans.⁵⁸ Nevertheless, the db/db mouse exhibits the most profound healing impairment relative to other diabetic mouse models,⁵⁹ as well as molecular similarities to human diabetic wounds⁶⁰ and has therefore been the mainstay of pre-clinical diabetic wound investigations.⁵⁸ Additionally, although

contraction is a major force in the healing of mouse skin human skin wound healing rather than the re-epithelialization that is the mechanism for healing in human skin, this difference is circumvented by the use of the well-established splinted wound healing model that restricts contraction.⁶¹

MSC persistence in the Integra scaffolds has been documented in our previous study and cell metabolism was measured by MTT assay.³⁵ The MSC cells are retained for 15 days in the scaffolds,³⁵ which coordinates with the wound healing period in this study. By using the splinted wound model in the impaired healing db/db mouse⁴⁸ and histological analysis of re-epithelialization to assess wound closure across the whole wound, the healing rates can be quantified accurately in this model, which is critical for designing the treatment regimens for clinical studies. We believe the 7-day time point in this impaired healing murine model to be the most predictive one for clinical utility, because at later time points in all murine mouse models of healing, the control and test wounds tend to reach similar endpoints. The continued application of topical timolol daily to the wound post MSC/T/H/S device implantation results in minimal systemic absorption and systemic accumulation of timolol. The detected timolol concentration in plasma is lower than 3 ng/mL, which is below the lowest plasma level (4-100 ng/mL) detected in test subjects after oral ingestion of 5 to 20 mg timolol⁶² that was associated with a decrease in heart rate. The combined protocol enhances the anti-inflammatory and pro-angiogenic functions and further improves on the pro-reparative abilities in the diabetic wounds in vivo.

The ultimate goal of this preclinical work is translation to patients with diabetic ulcers. There are no current US studies that are recruiting and propose to use allogeneic stem cells for treatment of diabetic ulcers, thus an unmet need to translate MSC wound protocols into the clinic.⁶³ The MSC/T/H/S device confers some advantages that will aid in its potential translation: it is a topical administered device, and incorporates bone marrow-derived MSC that have been very well characterized and already have a strong safety profile in the clinic.⁶⁴⁻⁶⁶ Having operational Standard Operating Procedures for handling the marrow-derived MSCs at the Good Manufacturing Practice facility can further expedite the translational process.

It is likely that a number of safety concerns will have to be addressed prior to full FDA approval of the MSC/T/H/S as Investigational New Drug. First, stem cell-based therapies for diabetic ulcers are considered to be cell transplantation in which tumorigenicity of the product is a possibility. Although MSC tumorigenicity is very rare event and has been reported only once in a long-term (>5 weeks) MSC culture,^{67,68} the concern can only be addressed pre-clinically in a large animal model to mimic the treatment regimens to be used in clinical trials. Long-term (8-12 weeks) treatment and monitoring of wounds similar to DFU sizes⁶⁹ (2.0-12.5 cm² DFU wounds, healing time from 7.2 to 8.8 weeks) in a large animal model, such as swine, and histo-pathological analysis of the wound tissue will help reveal if MSC application to the wound results in tumorigenicity. The skin architecture and healing process in swine closely resemble that of humans.⁷⁰ The porcine skin wound model is noted by the FDA as one

model of choice for preclinical efficacy in their guidelines for developing treatments for human chronic wounds,⁷¹ and porcine wound studies have a 78% concordance with human skin wound healing.⁷¹ Therefore, future assessment of wound healing and MSC retention after MSC/T/H/S in a swine wound model will provide insights to the design of the clinical treatments.

Second, there is a concern that the systemic levels of timolol dose applied to the wound may reach concentrations that could induce adverse effects, such as symptomatic bradycardia, wheezing, or orthostatic hypotension. The timolol dosage used in this study is extrapolated from the dosing recommendations for the commercially available 0.5% timolol solution for the treatment of glaucoma. Previous studies have shown that application of timolol solution to the ocular surface results in average plasma concentrations between 0.80 and 1.72 ng/mL with very little systemic effect,^{72,73} whereas orally administered 5 to 20 mg timolol for the treatment of hypertension produced plasma concentrations of 4 to 100 ng/mL.^{62,74,75} Because the concentrations we observed in mouse plasma were between 1 and 3 ng/mL, we do not anticipate any systemic effects due to timolol as a result of this treatment. Indeed, in a recent study comparing plasma levels of timolol in patients after ocular administration for glaucoma to those where timolol was administered topically to a chronic wound, no difference in levels were found, and almost all patient levels were in a range that is below that associated with adverse effects.⁷⁶ Timolol absorption from the short-term and long-term MSC/T/H/S treatments will need to be monitored in future continued large animal tests to generate a safety profile for the clinical studies.

5 | CONCLUSION

We demonstrate here a bioengineered device that combines hypoxia and timolol preconditioned MSC embedded within a dermal replacement extracellular matrix scaffold, and is demonstrated to promote wound healing in diabetic mice. Additional advantages of the combined device are enhanced anti-inflammatory and pro-angiogenic functions. We believe that this wound care device will be beneficial for the treatment of diabetic wounds and has the potential to be a valuable addition to improve healing in diabetic patients.

ACKNOWLEDGMENTS

This study was supported by the Preclinical Development Awards to R. Rivkah Isseroff and Jan A. Nolte (TR2-01787 and PC1-08118) from the California Institute for Regenerative Medicine (CIRM). CIRM fellows were funded by TB1-01184 and EDUC2-08390. Integra-Wound Matrix was provided by Integra LifeSciences.

CONFLICT OF INTEREST

Authors Mohan R. Dasu and R. Rivkah Isseroff have a pending patent application under review by USPTO. The other authors declared no potential conflict of interest.

AUTHOR CONTRIBUTIONS

H.Y., F.F., A.M.S.: conception and design, collection of data, data analysis and interpretation, manuscript writing; M.S.: collection of data, data analysis and interpretation; D.J.Y., M.D.B., T.R.C., A.A., H.S., M.C.: collection of data; A.V.N.: collection of data, data analysis and interpretation, manuscript writing; A.G., T.R.P.: collection of data, data analysis and interpretation; M.R.D.: conception and design; J.A.N., R.R.I.: conception and design, financial support, manuscript writing, final approval of manuscript.

DATA AVAILABILITY STATEMENT

The data that support the findings of this study are available on request from the corresponding author.

ORCID

Hsin-ya Yang  <https://orcid.org/0000-0002-5325-494X>

Alan Vu Nguyen  <https://orcid.org/0000-0002-2249-7244>

R. Rivkah Isseroff  <https://orcid.org/0000-0001-7813-0858>

REFERENCES

- American Diabetes Association. Economic costs of diabetes in the U.S. in 2012. *Diabetes Care*. 2013;36(4):1033-1046.
- Singh N, Armstrong DG, Lipsky BA. Preventing foot ulcers in patients with diabetes. *Jama*. 2005;293(2):217-228.
- Markowitz JS, Gutterman EM, Magee G, Margolis DJ. Risk of amputation in patients with diabetic foot ulcers: a claims-based study. *Wound Repair Regen*. 2006;14(1):11-17.
- Dietrich I, Braga GA, de Melo FG, da Costa Silva ACC. The diabetic foot as a proxy for cardiovascular events and mortality review. *Curr Atheroscler Rep*. 2017;19(11):44.
- Robbins JM, Strauss G, Aron D, Long J, Kuba J, Kaplan Y. Mortality rates and diabetic foot ulcers: is it time to communicate mortality risk to patients with diabetic foot ulceration? *J Am Podiatr Med Assoc*. 2008;98(6):489-493.
- Armstrong DG, Wrobel J, Robbins JM. Guest editorial: are diabetes-related wounds and amputations worse than cancer? *Int Wound J*. 2007;4(4):286-287.
- Kantor J, Margolis DJ. Treatment options for diabetic neuropathic foot ulcers: a cost-effectiveness analysis. *Dermatol Surg*. 2001;27(4):347-351.
- Margolis DJ, Kantor J, Berlin JA. Healing of diabetic neuropathic foot ulcers receiving standard treatment. A meta-analysis. *Diabetes Care*. 1999;22(5):692-695.
- Dinh T, Braunagel S, Rosenblum BI. Growth factors in wound healing: the present and the future? *Clin Podiatr Med Surg*. 2015;32(1):109-119.
- Lichtman MK, Otero-Vinas M, Falanga V. Transforming growth factor beta (TGF-beta) isoforms in wound healing and fibrosis. *Wound Repair Regen*. 2016;24(2):215-222.
- Dickinson LE, Gerecht S. Engineered biopolymeric scaffolds for chronic wound healing. *Front Physiol*. 2016;7:341.
- Rahmani Del Bakhshayesh A, Annabi N, Khalilov R, et al. Recent advances on biomedical applications of scaffolds in wound healing and dermal tissue engineering. *Artif Cells Nanomed Biotechnol*. 2018;46(4):691-705.
- NCT01060670 Cgl. A safety and efficacy study of INTEGRA® dermal regeneration template for the treatment of diabetic foot ulcers. <https://clinicaltrials.gov/ct2/show/study/NCT01060670?term=omnigraft+Integra&draw=2&rank=1>; 2016.

14. Driver VR, Lavery LA, Reyzelman AM, et al. A clinical trial of Integra template for diabetic foot ulcer treatment. *Wound Repair Regen.* 2015;23(6):891-900.
15. Nicholas MN, Yeung J. Current status and future of skin substitutes for chronic wound healing. *J Cutan Med Surg.* 2017;21(1):23-30.
16. Serra R, Rizzuto A, Rossi A, et al. Skin grafting for the treatment of chronic leg ulcers - a systematic review in evidence-based medicine. *Int Wound J.* 2017;14(1):149-157.
17. Zauyanov L, Kirsner RS. A review of a bi-layered living cell treatment (Apligraf) in the treatment of venous leg ulcers and diabetic foot ulcers. *Clin Interv Aging.* 2007;2(1):93-98.
18. Hart CE, Loewen-Rodriguez A, Lessem J. Dermagraft: use in the treatment of chronic wounds. *Adv Wound Care (New Rochelle).* 2012;1(3):138-141.
19. Caplan AI, Dennis JE. Mesenchymal stem cells as trophic mediators. *J Cell Biochem.* 2006;98(5):1076-1084.
20. Maxson S, Lopez EA, Yoo D, Danilkovitch-Miagkova A, Leroux MA. Concise review: role of mesenchymal stem cells in wound repair. *STEM CELLS TRANSLATIONAL MEDICINE.* 2012;1(2):142-149.
21. Chokesuwattanaskul S, Sukpat S, Duangpatra J, et al. High dose oral vitamin C and mesenchymal stem cells aid wound healing in a diabetic mouse model. *J Wound Care.* 2018;27(5):334-339.
22. Kim SW, Zhang HZ, Guo L, Kim JM, Kim MH. Amniotic mesenchymal stem cells enhance wound healing in diabetic NOD/SCID mice through high angiogenic and engraftment capabilities. *PLoS One.* 2012;7(7):e41105.
23. Yu B, Alboslemy T, Safadi F, Kim MH. Glycoprotein nonmelanoma clone B regulates the crosstalk between macrophages and mesenchymal stem cells toward wound repair. *J Invest Dermatol.* 2018;138(1):219-227.
24. Uchiyama A, Motegi SI, Sekiguchi A, et al. Mesenchymal stem cell-derived MFG-E8 accelerates diabetic cutaneous wound healing. *J Dermatol Sci.* 2017;86(3):187-197.
25. Vojtassak J, Danisovic L, Kubes M, et al. Autologous biograft and mesenchymal stem cells in treatment of the diabetic foot. *Neuro Endocrinol Lett.* 2006;27(Suppl 2):134-137.
26. Clinicaltrials.gov. 19 clinical trials were found on a search for "Diabetic Foot Ulcer, Mesenchymal Stem cell." Updated on October 4, 2019.
27. Ankrum JA, Ong JF, Karp JM. Mesenchymal stem cells: immune evasive, not immune privileged. *Nat Biotechnol.* 2014;32(3):252-260.
28. Lalu MM, McIntyre L, Pugliese C, et al. Safety of cell therapy with mesenchymal stromal cells (SafeCell): a systematic review and meta-analysis of clinical trials. *PLoS One.* 2012;7(10):e47559.
29. Borakati A, Mafi R, Mafi P, Khan WS. A systematic review and meta-analysis of clinical trials of mesenchymal stem cell therapy for cartilage repair. *Curr Stem Cell Res Ther.* 2018;13(3):215-225.
30. Jeremias Tda S, Machado RG, Visoni SB, Pereima MJ, Leonardi DF, Trentin AG. Dermal substitutes support the growth of human skin-derived mesenchymal stromal cells: potential tool for skin regeneration. *PLoS One.* 2014;9(2):e89542.
31. Hodgkinson T, Bayat A. Ex vivo evaluation of acellular and cellular collagen-glycosaminoglycan flowable matrices. *Biomed Mater.* 2015;10(4):041001.
32. Wahl EA, Fierro FA, Peavy TR, et al. In vitro evaluation of scaffolds for the delivery of mesenchymal stem cells to wounds. *Biomed Res Int.* 2015;2015:108571.
33. Cherubino M, Valdatta L, Balzaretto R, et al. Human adipose-derived stem cells promote vascularization of collagen-based scaffolds transplanted into nude mice. *Regen Med.* 2016;11(3):261-271.
34. Formigli L, Benvenuti S, Mercatelli R, et al. Dermal matrix scaffold engineered with adult mesenchymal stem cells and platelet-rich plasma as a potential tool for tissue repair and regeneration. *J Tissue Eng Regen Med.* 2012;6(2):125-134.
35. Fierro FA, O'Neal AJ, Beegle JR, et al. Hypoxic pre-conditioning increases the infiltration of endothelial cells into scaffolds for dermal regeneration pre-seeded with mesenchymal stem cells. *Front Cell Dev Biol.* 2015;3:68.
36. Beegle J, Lakatos K, Kalomoiris S, et al. Hypoxic preconditioning of mesenchymal stromal cells induces metabolic changes, enhances survival, and promotes cell retention in vivo. *STEM CELLS.* 2015;33(6):1818-1828.
37. Sivamani RK, Pullar CE, Manabat-Hidalgo CG, et al. Stress-mediated increases in systemic and local epinephrine impair skin wound healing: potential new indication for beta blockers. *PLoS Med.* 2009;6(1):e12.
38. Sivamani RK, Shi B, Griffiths E, et al. Acute wounding alters the beta2-adrenergic signaling and catecholamine synthetic pathways in keratinocytes. *J Invest Dermatol.* 2014;134(8):2258-2266.
39. Chen J, Hoffman BB, Isseroff RR. Beta-adrenergic receptor activation inhibits keratinocyte migration via a cyclic adenosine monophosphate-independent mechanism. *J Invest Dermatol.* 2002;119(6):1261-1268.
40. Pullar CE, Rizzo A, Isseroff RR. Beta-adrenergic receptor antagonists accelerate skin wound healing: evidence for a catecholamine synthesis network in the epidermis. *J Biol Chem.* 2006;281(30):21225-21235.
41. Pullar CE, Isseroff RR. Beta 2-adrenergic receptor activation delays dermal fibroblast-mediated contraction of collagen gels via a cAMP-dependent mechanism. *Wound Repair Regen.* 2005;13(4):405-411.
42. Pullar CE, Le Provost GS, O'Leary AP, Evans SE, Baier BS, Isseroff RR. beta2AR antagonists and beta2AR gene deletion both promote skin wound repair processes. *J Invest Dermatol.* 2012;132(8):2076-2084.
43. Kim MH, Liu W, Borjesson DL, et al. Dynamics of neutrophil infiltration during cutaneous wound healing and infection using fluorescence imaging. *J Invest Dermatol.* 2008;128(7):1812-1820.
44. Dasu MR, Ramirez SR, La TD, et al. Crosstalk between adrenergic and toll-like receptors in human mesenchymal stem cells and keratinocytes: a recipe for impaired wound healing. *STEM CELLS TRANSLATIONAL MEDICINE.* 2014;3(6):745-759.
45. Park SA, Covert J, Teixeira L, et al. Importance of defining experimental conditions in a mouse excisional wound model. *Wound Repair Regen.* 2015;23(2):251-261.
46. FDA. Timoptic drug label: https://www.accessdata.fda.gov/drugsatfda_docs/label/2006/018086s070s072lbl.pdf. 2006.
47. Nguyen CM, Tartar DM, Bagoood MD, et al. Topical fluoxetine as a novel therapeutic that improves wound healing in diabetic mice. *Diabetes.* 2019;68(7):1499-1507.
48. Park SA, Teixeira LB, Raghunathan VK, et al. Full-thickness splinted skin wound healing models in db/db and heterozygous mice: implications for wound healing impairment. *Wound Repair Regen.* 2014;22(3):368-380.
49. Gruenloh W, Kambal A, Sondergaard C, et al. Characterization and in vivo testing of mesenchymal stem cells derived from human embryonic stem cells. *Tissue Eng Part A.* 2011;17(11-12):1517-1525.
50. Oswald J, Boxberger S, Jorgensen B, et al. Mesenchymal stem cells can be differentiated into endothelial cells in vitro. *STEM CELLS.* 2004;22(3):377-384.
51. Mardpour S, Hamidieh AA, Taleahmad S, Sharifzad F, Taghikhani A, Baharvand H. Interaction between mesenchymal stromal cell-derived extracellular vesicles and immune cells by distinct protein content. *J Cell Physiol.* 2019;234(6):8249-8258.
52. Carr MW, Roth SJ, Luther E, Rose SS, Springer TA. Monocyte chemoattractant protein 1 acts as a T-lymphocyte chemoattractant. *Proc Natl Acad Sci USA.* 1994;91(9):3652-3656.
53. Xu LL, Warren MK, Rose WL, Gong W, Wang JM. Human recombinant monocyte chemotactic protein and other C-C chemokines bind and induce directional migration of dendritic cells in vitro. *J Leukoc Biol.* 1996;60(3):365-371.
54. Ishida Y, Kuninaka Y, Nosaka M, et al. CCL2-mediated reversal of impaired skin wound healing in diabetic mice by normalization of

- neovascularization and collagen accumulation. *J Invest Dermatol.* 2019;139:2517-2527.e5.
55. Schumacher C, Clark-Lewis I, Baggiolini M, Moser B. High- and low-affinity binding of GRO alpha and neutrophil-activating peptide 2 to interleukin 8 receptors on human neutrophils. *Proc Natl Acad Sci USA.* 1992;89(21):10542-10546.
 56. Wilkinson HN, Clowes C, Banyard KL, Matteucci P, Mace KA, Hardman MJ. Elevated local senescence in diabetic wound healing is linked to pathological repair via CXCR2. *J Invest Dermatol.* 2019;139(5):1171-1181.e1176.
 57. Nguyen AV, Soulika AM. The dynamics of the skin's immune system. *Int J Mol Sci.* 2019;20(8):1811. <https://doi.org/10.3390/ijms20081811>.
 58. Elliot S, Wikramanayake TC, Jozic I, Tomic-Canic M. A modeling conundrum murine models for cutaneous wound healing. *J Invest Dermatol.* 2018;138(4):736-740.
 59. Michaels Jt CSS, Blechman KM, et al. db/db mice exhibit severe wound-healing impairments compared with other murine diabetic strains in a silicone-splinted excisional wound model. *Wound Repair Regen.* 2007;15(5):665-670.
 60. Li X, Li D, Wang A, et al. MicroRNA-132 with therapeutic potential in chronic wounds. *J Invest Dermatol.* 2017;137(12):2630-2638.
 61. Wang X, Ge J, Tredget EE, Wu Y. The mouse excisional wound splinting model, including applications for stem cell transplantation. *Nat Protoc.* 2013;8(2):302-309.
 62. Bobik AJG, Ashley P, Korner PI. Timolol pharmacokinetics and effects on heart rate and blood pressure after acute and chronic administration. *Eur J Clin Pharmacol.* 1979;16(4):243-249.
 63. Clinicaltrials.gov. 159 clinical trials were found on a search of "Wound, Mesenchymal Stem cell". Updated on Oct. 4th, 2019.
 64. Hoogduijn MJ, Lombardo E. Concise review: mesenchymal stromal cells anno 2019: dawn of the therapeutic era? *STEM CELLS TRANSLATIONAL MEDICINE.* 2019;8:1126-1134.
 65. Viswanathan S, Shi Y, Galipeau J, et al. Mesenchymal stem versus stromal cells: International Society for Cellular Therapy Mesenchymal Stromal Cell committee position statement on nomenclature. *Cytotherapy.* 2019;21:1019-1024.
 66. Andrzejewska A, Lukomska B, Janowski M. Concise review: mesenchymal stem cells: from roots to boost. *STEM CELLS.* 2019;37(7):855-864.
 67. Pan Q, Fouraschen SM, de Ruiter PE, et al. Detection of spontaneous tumorigenic transformation during culture expansion of human mesenchymal stromal cells. *Exp Biol Med (Maywood).* 2014;239(1):105-115.
 68. Neri S. Genetic stability of mesenchymal stromal cells for regenerative medicine applications: a fundamental biosafety aspect. *Int J Mol Sci.* 2019;20(10):2406. <https://doi.org/10.3390/ijms20102406>.
 69. Babaei V, Afradi H, Gohardani HZ, Nasser F, Azarafza M, Teimourian S. Management of chronic diabetic foot ulcers using platelet-rich plasma. *J Wound Care.* 2017;26(12):784-787.
 70. Lindblad WJ. Considerations for selecting the correct animal model for dermal wound-healing studies. *J Biomater Sci Polym Ed.* 2008;19(8):1087-1096.
 71. Sullivan TP, Eaglstein WH, Davis SC, Mertz P. The pig as a model for human wound healing. *Wound Repair Regen.* 2001;9(2):66-76.
 72. Uusitalo H, Kahonen M, Ropo A, et al. Improved systemic safety and risk-benefit ratio of topical 0.1% timolol hydrogel compared with 0.5% timolol aqueous solution in the treatment of glaucoma. *Graefes Arch Clin Exp Ophthalmol.* 2006;244(11):1491-1496.
 73. Uusitalo H, Nino J, Tahvanainen K, et al. Efficacy and systemic side-effects of topical 0.5% timolol aqueous solution and 0.1% timolol hydrogel. *Acta Ophthalmol Scand.* 2005;83(6):723-728.
 74. Fourtillan JB, Courtois P, Lefebvre MA, Girault J. Pharmacokinetics of oral timolol studied by mass fragmentography. *Eur J Clin Pharmacol.* 1981;19(3):193-196.
 75. Wilson TW, Firor WB, Johnson GE, et al. Timolol and propranolol: bioavailability, plasma concentrations, and beta blockade. *Clin Pharmacol Ther.* 1982;32(6):676-685.
 76. Gallegos AC, Davis MJ, Tchanque-Fossuo CN, et al. Absorption and safety of topically applied timolol for treatment of chronic cutaneous wounds. *Adv Wound Care (New Rochelle).* 2019;8(11):538-545.

SUPPORTING INFORMATION

Additional supporting information may be found online in the Supporting Information section at the end of this article.

How to cite this article: Yang H, Fierro F, So M, et al.

Combination product of dermal matrix, human mesenchymal stem cells, and timolol promotes diabetic wound healing in mice. *STEM CELLS Transl Med.* 2020;1-12. <https://doi.org/10.1002/sctm.19-0380>